Paper 261

©Civil-Comp Press, 2012
Proceedings of the Eleventh International Conference
on Computational Structures Technology,
B.H.V. Topping, (Editor),
Civil-Comp Press, Stirlingshire, Scotland

Strain Behaviour of Concrete subjected to Combined Mechanical and Thermal Loading: From Micromechanical Modelling to Simulation of Real-Scale Fire Tests

T. Ring[1], M. Zeiml[1,3] and R. Lackner[2]
[1] Institute for Mechanics of Materials and Structures (IMWS)
Vienna University of Technology, Austria
[2] Material-Technology Innsbruck (MTI), University of Innsbruck, Austria
[3] Fritsch, Chiari & Partner ZT GmbH, Vienna, Austria

Abstract

In this paper, the strain behavior of concrete under combined thermal and mechanical loading is investigated. Under these loading conditions, concrete exhibits a certain path dependence explained by the dependence of physical processes on the actual stress state within concrete. In the literature, this path dependence is often referred to as load-induced thermal strains (LITS). In this paper, a micromechanics-based model for the effective material properties and free thermal strain of concrete under fire loading is introduced for modeling of LITS and applied in the context of simulation of real-scale structures, highlighting the influence of LITS on the structural response.

Keywords: concrete, fire, experiment, thermal strain, micromechanical modeling.

1 Introduction

Concrete subjected to concrete under combined mechanical and thermal loading exhibits a certain path dependence explained by the dependence of physical processes on the actual stress state within the material (see (1; 3; 5; 7; 11; 20; 21; 23)). This path dependence of heated concrete (highlighted in Figure 1) is often related to the introduction of so-called load induced thermal strains (LITS). The main findings reported in the literature with respect to LITS are:

1. LITS is found only in concrete subjected to first thermal loading (7).
2. The rate of heating (ranging from 0.2 to 5 °C/min) and the water/cement-ratio showed only minor influence on LITS (20).
3. The aggregate type has no significant influence in the development of LITS, linking LITS to processes taking place within the cement paste (7).

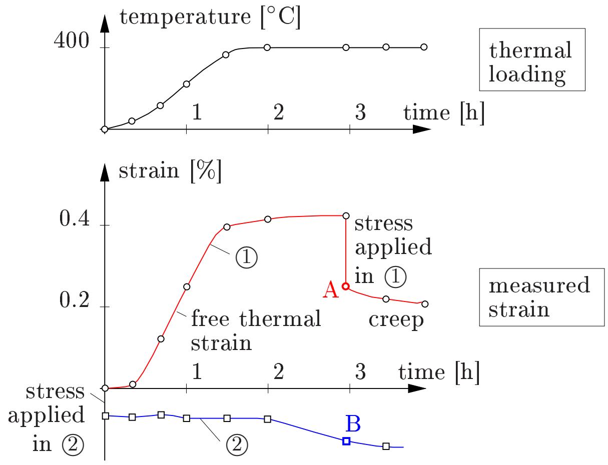

Figure 1: Path dependence of concrete under combined mechanical and thermal loading according to (22); (The same thermal loading and the same mechanical loading applied differently lead to the same temperature and stress level ($T_{max} = 400$ °C and $\sigma = 0.45 f_{c,0}$) but to different experimentally-observed strains – compare points A and B.)

4. LITS is practically unaffected by the type of cement blend, suggesting that it takes place in a common gel or CSH structure (7).

5. LITS seems to increase linearly with the applied stress level (see Figure 2) (1).

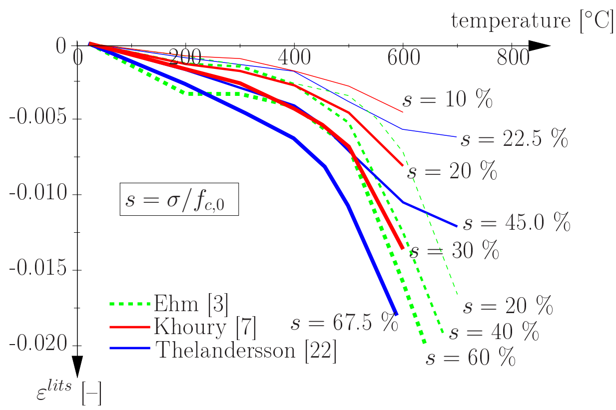

Figure 2: Load dependency of LITS obtained from different experiments (3; 7; 22) ($s = \sigma/f_{c,0}$: level of loading)

Based on these experimental findings, several formulations for LITS can be found in the open literature, ranging from an approach to model LITS within creep of heated concrete (20), considering LITS via empirical relations (21), to strain-rate formulations for LITS as proposed in (11; 22).

In recent years, micromechanics-based models for concrete have been published in the open literature, e.g., (2; 9), taking the composite nature of concrete into account. On the one hand, these models were developed in order to identify the behavior of C-S-H at elevated temperatures (2) using nanoindentation. On the other hand, a multi-scale model for determination of the effective stiffness of concrete at high temperatures was proposed in (9).

In the present work, recently published micromechanics-based models (8; 13) are adopted to the description of the change of elastic properties and the thermal dilation of heated concrete. For this purpose, experimental studies on concrete and cement-paste samples were conducted, with the respective experimental results given in Section 2. In Section 3, the micromechanics-based model is presented with a possible mode of implementation of the underlying stress-strain behavior into a numerical analysis tool. The so-obtained formulation for consideration of the combined thermo-mechanical behavior of concrete and its effect within the analysis of concrete structures subjected to fire loading is highlighted in Section 4. Finally, concluding remarks are given in Section 5.

2 Experimental observations

A radiant electric oven (see Figure 3) was used to conduct the experiments on concrete specimens (with a diameter of 100 mm and a height of 200 mm). The test setup allows to test specimens under combined uniaxial mechanical and thermal loading (see (18) for details). The deformations are transferred with steel bars to the outside of the oven, giving access to the axial and radial deformations. In order to determine the material properties (Young's modulus E and Poisson's ration ν), small load changes were applied to the specimen, giving access to the load- and temperature-dependent evolution of these properties.

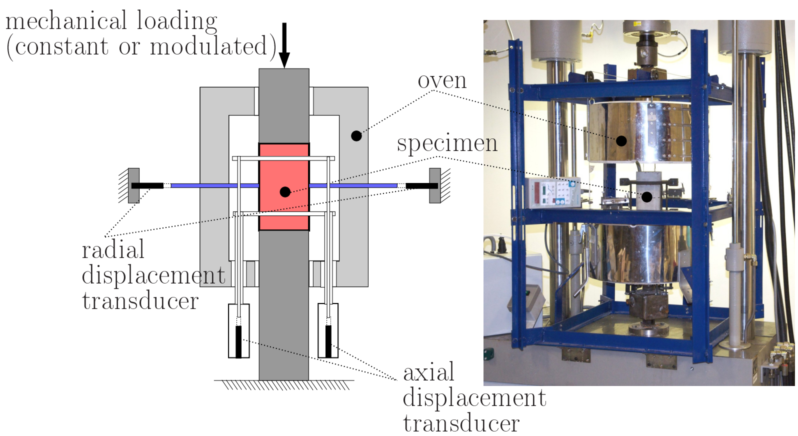

Figure 3: Test setup for combined thermal and mechanical testing (18)

In the following, the experimental results (strain behavior and material properties) for concrete are presented (the full set of experimental data can be found in (18), including experimental data for cement-paste specimens). In Figure 4, the evolution of axial and radial strain for concrete specimens subjected to different mechanical load levels s is presented ($s = 0$ to 60 % with $s = 100\sigma_a/f_{c,0}$, with the initial compressive strength $f_{c,0} = 39.1$ MPa). With increasing load level, a decrease of axial strain is observed, whereas the corresponding radial strain increases.

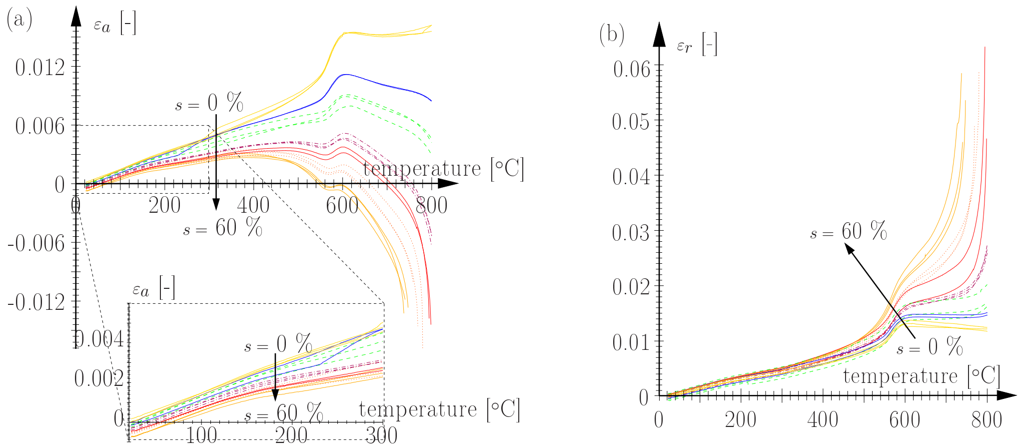

Figure 4: Strain of concrete without PP-fibers under combined thermal (up to 800 °C) and mechanical loading ($s = 0$ to 60 % with $s = 100\sigma_a/f_{c,0}$, where $f_{c,0} = 39.1$ MPa): evolution of (a) axial and (b) radial strain as a function of temperature (18)

The load-dependency of the elastic parameters for concrete is shown in Figure 5, revealing an increase of stiffness in case of mechanically preloaded specimens which can be explained by the reduced amount of microcracking originating from thermal expansion/degradation. The evolution of Poisson's ratio shows similar behavior up to 400 °C, followed by an increase for higher temperatures and mechanical load levels.

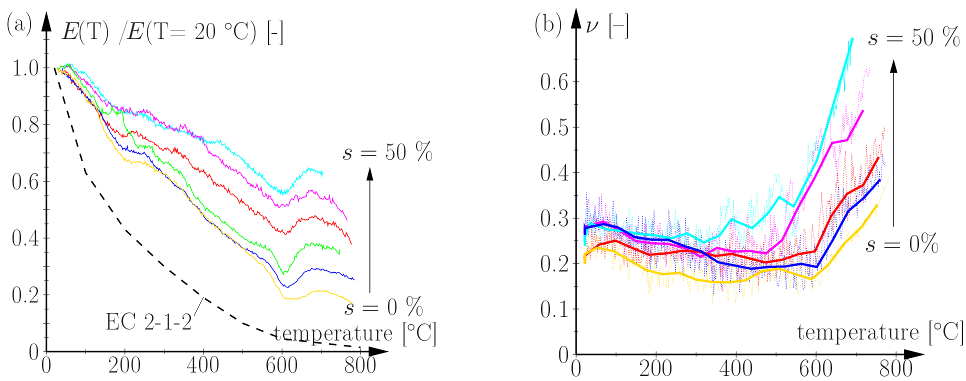

Figure 5: Elastic parameters of specimens made of concrete without PP-fibers for different load levels ($s = 0$ to 50 %): evolution of (a) normalized Young's modulus compared to EC2-1-2 (4) and (b) Poisson's ratio as a function of temperature (18)

3 Micromechanical model

The proposed micromechanical model (15) consists of two scales (see Figure 6), in order to take the influence of the concrete constituents (aggregate, cement paste, pore space) into account. Scale I consists of the cement-paste composite (pore space, hydration products) and additional pore space, introduced during the mixing process of concrete. At Scale II, aggregates are added to the homogenized material from Scale I. For the proposed micromechanical model, both the effective elastic and thermal-dilation properties of heated concrete are determined using continuum micromechanics (based on (10), applied in (8; 12)).

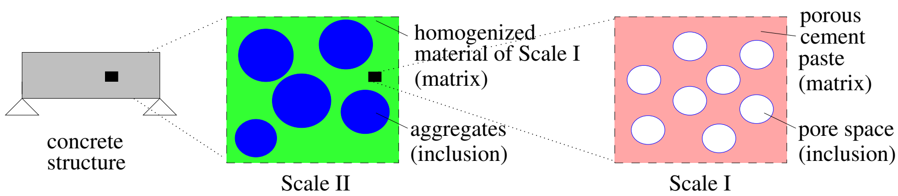

Figure 6: Micromechanical model for high-temperature concrete proposed in (15)

3.1 Effective elastic properties

The effective shear and bulk modulus, G_{eff} [MPa] and K_{eff} [MPa], are given as:

$$G_{eff} = \frac{\displaystyle\sum_r f_r G_r \left[1 + \beta \left(\frac{G_r}{G_m} - 1\right)\right]^{-1}}{\displaystyle\sum_r f_r \left[1 + \beta \left(\frac{G_r}{G_m} - 1\right)\right]^{-1}} \tag{1}$$

and

$$K_{eff} = \frac{\displaystyle\sum_r f_r K_r \left[1 + \alpha \left(\frac{K_r}{K_m} - 1\right)\right]^{-1}}{\displaystyle\sum_r f_r \left[1 + \alpha \left(\frac{K_r}{K_m} - 1\right)\right]^{-1}}\,, \tag{2}$$

with $r \in \{$porous cement paste (matrix), additional pore space (inclusion)$\}$ at Scale I and $r \in \{$homogenized material of Scale I (matrix), aggregates (inclusion)$\}$ at Scale II, where m refers to the matrix phase. In Equations (1) and (2), α and β represent the volumetric and deviatoric part of the Eshelby tensor $\mathbb{S}$, specialized for the case of spherical inclusions, reading

$$\alpha = \frac{3K_m}{3K_m + 4G_m} \quad \text{and} \quad \beta = \frac{6(K_m + 2G_m)}{5(3K_m + 4G_m)}\,, \tag{3}$$

where K_m and G_m refer to the bulk and shear modulus of the matrix phase, respectively, and f_r [–] is the volume fraction of the r-th material phase (see (15) for details).

3.2 Effective thermal strain

The effective thermal strain, based on (8), is given by

$$\varepsilon^{th}_{eff} = \varepsilon^{th}_m + (1 - f_m \langle A \rangle_{Vm}) \frac{K_i}{K_{eff}} (\varepsilon^{th}_i - \varepsilon^{th}_m) \, , \tag{4}$$

where ε^{th}_i and K_i are the thermal strain and bulk modulus of the inclusion phase i (additional pore space at Scale I, aggregates at Scale II), respectively. Furthermore, the index m refers to the respective matrix phase. Figure 7 contains the evolution of the effective thermal strain obtained from the proposed micromechanical model, showing excellent agreement with the experimental observations. As indicated in Figure 7, the free thermal strain is mainly driven by the behavior of the aggregates.

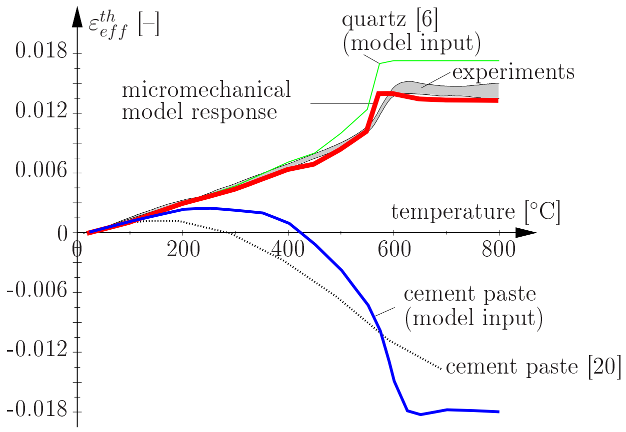

Figure 7: Free thermal strain ($s = 0$ %) of concrete predicted by the micromechanical model compared to the experimentally-obtained thermal strain (aggregates (6) and cement paste (20), see (15) for details)

3.3 Total formulation of LITS

For the formulation of LITS, the aforementioned micromechanically-determined material parameters are employed. LITS is considered by introducing an additional strain, ε_{lits} [–], giving the total strain ε^{tot} [–] as

$$\varepsilon^{tot} = \varepsilon^{el}(T, \sigma) + \varepsilon^{th}(T) + \varepsilon^{lits}(T, \sigma) \, , \tag{5}$$

where ε^{el} and ε^{th} represent the elastic strain and the free thermal strain (ε^{th} is taken from the micromechanical model, see Figure 7), respectively. In (15), the stress-dependence of LITS introduced in Equation (5) is considered by a modified approach based on the model proposed by Thelandersson (22):

$$\varepsilon^{lits} = k \frac{\sigma}{f_c(T)} \varepsilon^{th}(T) \,, \tag{6}$$

where k is a parameter depending on the type of loading (given in (22) as $k = 2.35$ for uniaxial loading, $k = 1.7$ for biaxial loading, whereas $k = 0.4$ is chosen in the current approach) and $\sigma/f_c(T)$ accounts for the influence of the load level, where $f_c(T)$ is the temperature-dependent compressive strength of concrete. The respective model response in comparison to the axial-strain curves obtained from experiments (see Figure 4(a)) shows good agreement (see Figure 8).

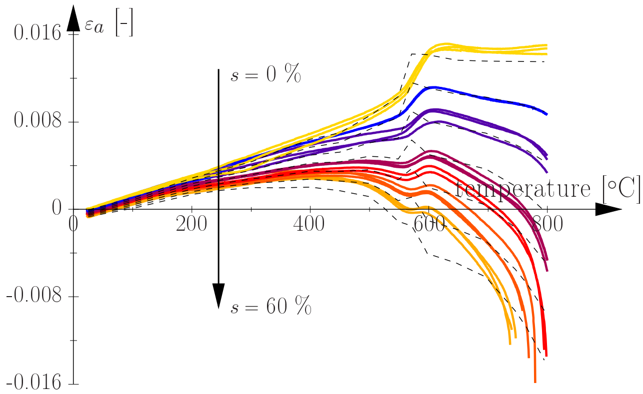

Figure 8: Evolution of axial strain of concrete: Modified total formulation compared with experimental data (15)

4 Structural model response

In (17), the influence of the strain behavior in consequence of combined mechanical and thermal loading (LITS) on the structural response was investigated on a large-scale structure (see Figure 9).

Real-scale fire tests were performed (see (14; 16) for details), collecting experimental data like temperature, spalling behavior, deformations, and rotations, in order to allow proper validation of numerical analysis tools. Such a tool departing from the one described in (19) was used for consideration of the proposed LITS model.

In Figure 10, selected results from (17) are presented, highlighting the influence of LITS on the deformations of a reinforced-concrete structure. The model response of the frame in the plane of symmetry is compared to experimental results, showing better agreement with the experimental data in case LITS in considered.

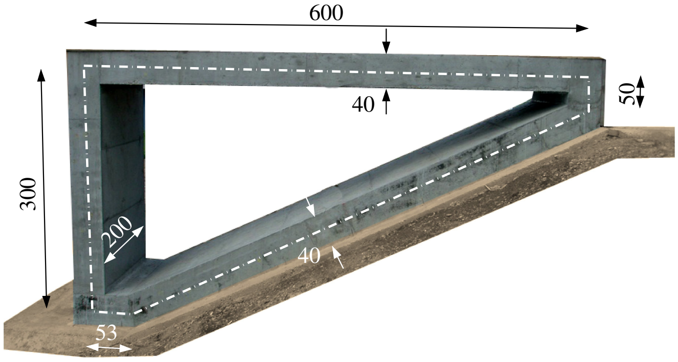

Figure 9: Experimentally-investigated concrete structure (16)

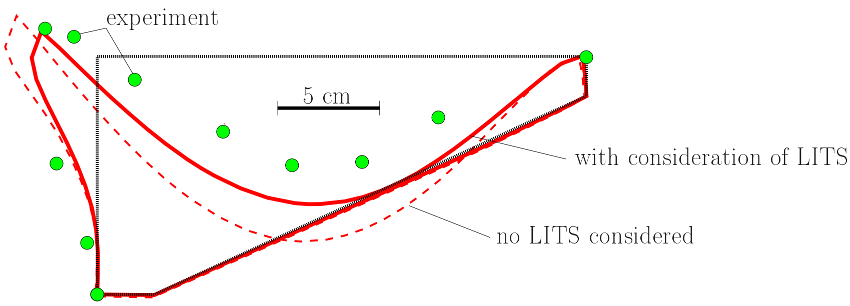

Figure 10: Deformations at plane of symmetry for $t_{fire} = 180$ min compared with experimental data (see (17), for details)

5 Concluding remarks

Starting with an experimental program comprising concrete and cement-paste samples, the main mechanisms in heated concrete were identified. In these experiments, cylindrical specimens with a diameter of 100 mm and a height of 200 mm were tested. These specimens were subjected to constant uniaxial (mechanical) loading and heated up to 800 °C with a heating rate of 1 °C/min. During the experiment, both the radial and axial deformations of the specimens were monitored, yielding the axial and radial strains of heated concrete. Moreover, the elastic properties of heated concrete and cement paste under various load levels were determined, applying an oscillating mechanical loading.

In order to consider the complex chemical and physical processes in heated concrete, a micromechanical model, taking the composite nature of concrete (consisting of aggregates, cement paste, pores) into account, was proposed, using the Mori-Tanaka scheme (10) for homogenization. Based on the aforementioned experimental data, the macroscopic behavior of concrete was determined. Comparing the model response with the collected experimental data shows good agreement. To describe the combined thermo-mechanical behavior of thermal strains (LITS) a modified approach based on the one based on Thelandersson (22) was developed (see (15) for details).

Finally, the micromechanical model developed was implemented – using a total formulation for the strain evolution of heated concrete – into a finite-element program (19). With this numerical tool at hand, validation simulations were performed, comparing the numerical results to experimental data from large-scale fire tests on concrete frames (length x height x depth: 6 x 3 x 2 m, see (16; 17), for details). Consideration of LITS within the material model was found to reduce thermal restraint and give improved agreement with experimental results, providing the basis for realistic structural safety assessment and, therefore, for a more economic design of concrete structures subjected to fire loading.

Acknowledgment

This research was conducted with financial support by the Austrian Ministry for Transport, Innovation and Technology (bm.vit) within the KIRAS project (Austrian security research program) 824781 ”Sicherheit von Hohlraumbauten unter Feuerlast – Entwicklung eines Struktursimulationstools (Safety of underground structures under fire loading – Development of a structural simulation tool)”.

References

[1] Y. Anderberg, S. Thelandersson, “Stress and deformation characteristics of concrete at high temperatures: 2. experimental investigation and material behaviour model”, Technical Report 54, Lund Institute of Technology, Lund, 1976.

[2] M.J. DeJong, F.J. Ulm, “The nanogranular behavior of C-S-H at elevated temperatures (up to 700 °C)”, *Cement and Concrete Research*, 37: 1–12, 2007.

[3] C. Ehm, *Versuche zur Festigkeit und Verformung von Beton unter zweiaxialer Beanspruchung und hohen Tempearturen [Experiments on strength and strain of concrete under biaxial loading at high temperatures*, PhD thesis, University of Braunschweig, Braunschweig, Germany, 1985.

[4] EN1992-1-2, *Eurocode 2 – Bemessung und Konstruktion von Stahlbeton- und Spannbetontragwerken – Teil 1-2: Allgemeine Regeln – Tragwerksbemessung für den Brandfall [Eurocode 2 – Design of concrete structures – Part 1-2: General rules – Structural fire design]*, European Committee for Standardization (CEN), 2007, In German.

[5] D. Gawin, F. Pesavento, B.A. Schrefler, “Modelling of deformations of high strength concrete at elevated temperatures”, 37: 218–236, 2004.

[6] A.H. Jay, “The thermal expansion of Quartz by X-ray measurements”, *Proceedings of the Royal Society of London*, pages 227–247, 1933.

[7] G.A. Khoury, B.N. Grainger, P.J.E. Sullivan, “Strain of concrete during first heating to 600°C”, *Magazine of Concrete Research*, 37(133): 195–215, 1985.

[8] R. Lackner, C. Pichler, A. Kloiber, "Artificial ground freezing of fully saturated soil: Viscoelastic behavior", *Journal of Engineering Mechanics (ASCE)*, 134 (1): 1–11, 2008.

[9] J. Lee, Y. Xi, K. Willam, Y. Jung, "A multiscale model for modulus of elasticity of concrete at high temperatures", *Cement and Concrete Research*, 39: 754–762, 2009.

[10] T. Mori, K. Tanaka, "Average stress in matrix and average elastic energy of materials with misfitting inclusions", *Acta Metallurgica*, 21: 571–574, 1973.

[11] C.V. Nielsen, C.J. Pearce, N. Bićanić, "Improved phenomenological modelling of transient thermal strains for concrete at high temperatures", *Computers and Concrete*, 1(2): 189–209, 2004.

[12] C. Pichler, *Multiscale characterization and modeling of creep and autogenous shrinkage of early-age cement-based materials*, PhD thesis, Vienna University of Technology, Juni 2007.

[13] C. Pichler, R. Lackner, "A Multiscale Micromechanics Model for Early-Age Basic Creep of Cement-Based Materials", *International Journal of Computers and Concrete*, 5(4): 295–328, 2008.

[14] T. Ring, M. Zeiml, R. Lackner, "Brandversuche zum Abplatz- und Strukturverhalten von Tunnel mit Rechtecksquerschnitt", Technical report, Vienna University of Technology, Vienna, Austria, 2012, In German.

[15] T. Ring, M. Zeiml, R. Lackner, "Thermo-mechanical behavior of concrete at high temperature: From micromechanical modeling towards tunnel safety assessment", *Cement and Concrete Research*, 2012, Submitted for publication.

[16] T. Ring, M. Zeiml, R. Lackner, "Underground concrete frame structures subjected to fire loading: Part I – Large scale fire tests", *Engineering Structures*, 2012, Submitted for publication.

[17] T. Ring, M. Zeiml, R. Lackner, "Underground concrete frame structures subjected to fire loading: Part II – re-analysis of large-scale fire tests", *Engineering Structures*, 2012, Submitted for publication.

[18] T. Ring, M. Zeiml, R. Lackner, J. Eberhardsteiner, "Experimental investiagtion of strain behavior of heated cement paste and concrete", *Strain*, 2012, Submitted for publication.

[19] K. Savov, R. Lackner, H.A. Mang, "Stability assessment of shallow tunnels subjected to fire load", *Fire Safety Journal*, 40: 745–763, 2005.

[20] U. Schneider, "Concrete at high temperature – a general review", *Fire Safety Journal*, 13: 55–68, 1988.

[21] M.J. Terro, "Numerical Modeling of the behavior of concrete structures in fire", *ACI Structural Journal*, 95(2): 183–193, 1998.

[22] S. Thelandersson, "Modeling of combined thermal and mechanical action in concrete", *Journal of Engineering Mechanics (ASCE)*, 113(6): 893–906, 1987.

[23] K.C. Thienel, "Festigkeit und Verformung von Beton bei hoher Temperatur und biaxialer Beanspruchung – Versuche und Modellbildung [Strength and strain of concrete at high temperature – experiments and modeling]", Technical Report 437, Deutscher Ausschuss für Stahlbeton, Berlin, 1994.